Adsorption 11: 295–299, 2005

Sublimation Phenomena in Slit Nanopores: Lennard-Jones Phase Diagram

HIDEKI KANDA*
Energy Engineering Research Laboratory, Central Research Institute of Electric Power Industry, Yokosuka, Kanagawa 240-0196, Japan
kanda@criepi.denken.or.jp

MINORU MIYAHARA AND KO HIGASHITANI
Chemical Engineering Department, Kyoto University, Kyoto 615-8510, Japan

Abstract. Sublimation phenomena of Lennard-Jones fluids in slit-shaped nanopores were examined. Vapor-phase pressure at which a solid phase forms in a pore at a constant temperature is determined by the authors' molecular dynamics technique. The obtained phase-boundary pressure is remarkably lower than that of the bulk phase. A simple model of the sublimation is presented, which successfully predicts the molecular dynamics results with no adjustable parameter. Thus, a whole Lennard-Jones phase diagram in slit-shaped nanopores can now be predicted.

Keywords: vapor-solid equilibria, nanopore, phase transition, Lennard-Jones, molecular simulation

1. Introduction

Phase transitions in confined nanospace have been much studied theoretically and experimentally (e.g., Patrik and Kemper, 1938). As for capillary condensation (vapor-liquid coexistence), many studies have pointed out the incorrectness of the Kelvin model at the nanometer scale. A condensation model of Lennard-Jones (LJ) fluid with a simple concept and easy calculation, however, had not been established until done recently by the present authors in computer experiments employing Molecular Dynamics (MD) techniques (Miyahara et al., 1997, 2000a; Kanda et al., 2000a). The model successfully predicted the real pore size of a mesoporous material through N_2 adsorption, and proved its reliability in a real experimental system with no adjustable parameter (Kanda et al., 2000c).

Also, as for freezing phenomena (solid-liquid coexistence), the present authors have clarified various shifts in freezing point. Freezing-point temperature was found to become higher as well as lower than the bulk freezing point, which is thought to have resulted from the combination of three factors: (i) the elevating effect by the pore-wall potential energy (compressing effect) (Miyahara and Gubbins, 1997), (ii) geometrical shape of pore (geometrical hindrance effect) (Maddox and Gubbins, 1997; Kanda et al., 2000b), and (iii) the depressing effect by the tensile condition of the capillary condensate (tensile effect) (Miyahara et al., 2000a). The authors' simple solidification models of LJ fluid successfully predicted simulation results of Grand Canonical Monte Carlo (GCMC) and MD. Further, triple points of pore fluid can be estimated as the simultaneous solution of our model of vapor-liquid coexistence and that of solid-liquid coexistence, which successfully predicted MD results again with no adjustable parameter (Kanda et al., 2004).

In this research, we examine sublimations of LJ fluid in slit nanopores. We employed an MD technique in a unit cell with an imaginary gas phase developed by the authors. This technique enabled us to set or obtain the equilibrium vapor-phase pressure for an adsorbed phase in a pore. For various number densities of LJ particles in a pore, corresponding vapor pressures are traced with the information of phase conditions in the pore to determine a phase-boundary vapor pressure

*To whom correspondence should be addressed.

for sublimation. Our simple model of the sublimation point successfully predicts the simulation results with no need to introduce any adjustable parameters, and is thus reliable.

2. MD Technique Capable of Simulation of Both Intra-Pore Solid and Extra-Pore Vapor

A unit cell, developed earlier by the authors, was used in an NVT-MD simulation, as shown in Fig. 1. Using this unit cell, the authors were able to calculate the vapor pressure outside the pore in equilibrium with pore fluid. Readers are referred to our earlier papers (Miyahara et al., 1997, 2000a, 2000b; Kanda et al., 2004) for details of the cell; the following is merely a summary about the cell.

In the middle of the cell is the pore space with a given potential energy (full potential field: FPF). Almost all the particles exist in this field. At each end of the cell, we set a border plane with an imaginary vapor phase. The external potential energy in the vapor phase must be zero, and therefore a connecting space with slope of potential energy (potential buffering field: PBF) should exist between the gas phase and the pore space. If we set a perfect reflection condition at the border, the equilibrium vapor-phase pressure can be calculated by counting the frequency of the particles that are able to escape from the attraction of the pore and reach the imaginary vapor phase.

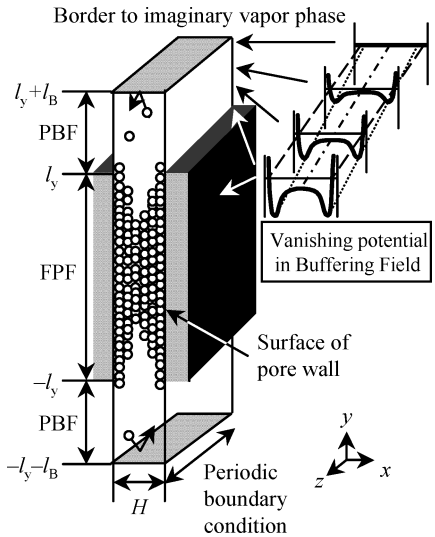

Figure 1. Unit cell with imaginary gas phase.

The fluid employed in this simulation was modeled on truncated and shifted LJ methane ($\varepsilon/k = 148.1$ K, $\sigma = 0.381$ nm). The cutoff distance was set to 5σ. The mass of the methane was 2.664×10^{-26} kg. Structureless 10-4-3 LJ graphite was used for each pore wall. The Lorentz–Berthelot combining rules were applied to obtain parameters for the methane–graphite interactions. The pore width H was 9.5σ. The length of the pore wall $2l_y$ was set to $7H$ to enable a solid phase of sufficient thickness to be created inside the pore. The PBF length was set to 13.12σ, which was sufficiently long so that particles near the border plane were not affected by pore fluid. The cell length in the z-direction was 10σ and we imposed periodic boundary conditions in the z-direction.

The total interaction energy that a particle i receives inside the FPF is the sum of the interaction energy from other particles, plus the superposition of the interaction energy from the two pore walls. In the PBF, interaction energy from the walls was attenuated linearly, from the inside of the pore towards the border of the imaginary vapor phase. The initial velocity of each particle was given so as to attain the Maxwell-Boltzmann distribution at a given temperature. The temperature of the system was controlled by temperature scaling once every 100 steps, during 1000 ps in the beginning. The Leapfrog Verlet method was used to integrate the particles' equations of motion with time increments of 10 fs. Each simulation was run until the number of particles that had arrived at the imaginary vapor phase was about 500 or more. The vapor phase pressure outside the pore was then determined.

To determine a vapor-solid phase boundary, simulation runs were performed with various numbers of particles at the temperature of 101.7 K, which is lower than the triple point for the fluid in this pore. Obtaining equilibrium vapor pressures for the runs, an isotherm can then be drawn. A transition between a vapor state (or a surface adsorption state) and a solid state (or a capillary condensed state) indicates the phase boundary. A simulation run for a given number of fluid particles started from an initial configuration arranged as a liquid-like phase within the slit-shaped pore. The total number of particles N ranged from approximately 2000 to 5500 depending on the desired pressure.

3. Results and Discussion

Figure 2 shows typical snapshots of LJ-methane in graphite pores at various equilibrium vapor pressures.

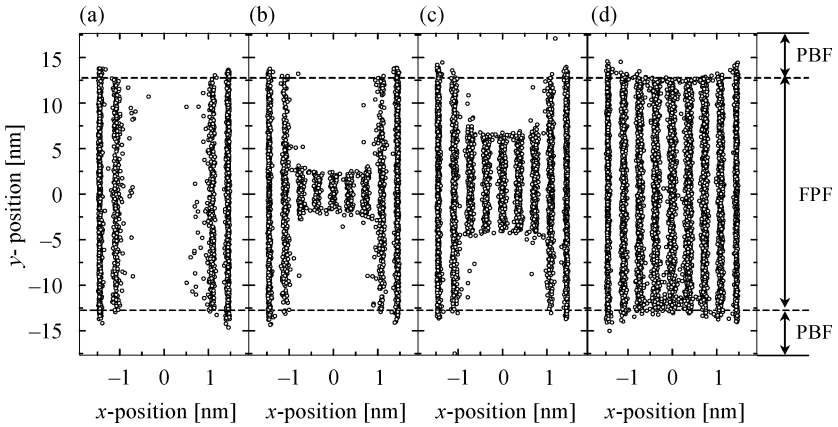

Figure 2. Snapshots of sublimation phenomena within a pore of $H = 9.5$ s: $T = 101.7$ K. (a) $p = 0.074$ atm, $N = 2000$, (b) $p = 0.114$ atm, $N = 2500$, (c) $p = 0.118$ atm, $N = 3500$, (d) $p = 0.196$ atm, $N = 5500$.

In the figure, note that the x-scale of each figure is expanded 5 times for ease of recognition of layers of pore fluids. At a lower pressure (Fig. 2(a)), there is no condensate but surface-adsorbed molecules. Near the sublimation pressure (Fig. 2(b)), the pore fluid exhibits sublimation, which is similar to capillary condensate typically observed at a higher temperature. In Fig. 2(c), only a slight difference in vapor pressure leads to thickening of the frozen condensate, but the vapor phase still exists in FPF. Further increases in equilibrium pressure cause essentially no change in the state of molecules as seen in Fig. 2(d). Under saturated vapor the system is solid-like at this temperature, and the above variation seems quite reasonable.

The average densities of the fluid in pores at the central portion of the cell were evaluated from the data after 2000 ps, and plotted against the relative pressures in Fig. 3. Open circles show the surface adsorption, and closed circles the solid state. An almost vertical change in the density can be recognized. The sublimation pressures can be determined from the rise of the isotherm: the above difference between Fig. 2(b) and (c) clearly demonstrates that the change around $p/p_s = 0.276$ ($p = 0.116$ atm) is associated with vapor-solid phase transition.

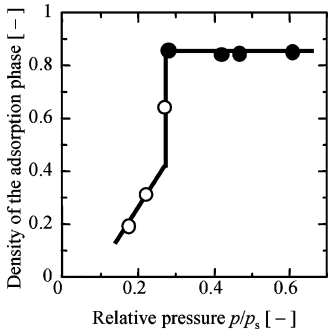

Figure 3. Adsorption isotherm obtained with MD simulations. Open circles show the surface adsorption, and closed circles the solid state. The vertical line indicates the solid-vapor coexistence condition.

Here we examine to what extent a simple concept can model the sublimation phenomenon observed above. As a starting point of a sublimation coexistence curve, we take the triple point of pore fluid (point A in Fig. 5), which is given by the following equations. For details, refer to the authors' previous paper (Kanda et al., 2004).

$$T|_A - T_a = \left(-\frac{\gamma_{\mathrm{gl}}}{\rho(x)} + \frac{\Delta\psi(x)}{v_L}\right)\left(\frac{\Delta v}{\Delta s}\right)_{\mathrm{bulk}} \quad (1)$$

$$p|_A = p_{\mathrm{s}}(T|_A)\exp\left[\left(\frac{\Delta s}{\Delta v}\right)_{\mathrm{bulk}} \frac{v_L}{kT|_A}(T|_A - T_a)\right] \quad (2)$$

where T is temperature and p is the equilibrium vapor-phase pressure. T_a is the freezing temperature under the saturated pressure $p_s(T_a)$, which is predicted by the equation proposed by Miyahara and Gubbins (1997). γ_{gl} is the surface tension of a liquid with a curved interface (Tolman, 1948; Kirkwood and Buff, 1949; Melrose, 1968) and $\rho(x)$ is the local radius of principal curvature of the vapor-liquid interface of condensate at a pore width position x. $\Delta\psi(x)$ is the contribution of the excess potential energy from the pore wall. v_L is the volume per molecule of the bulk liquid. Δv is the difference in molar volume between solid and liquid,

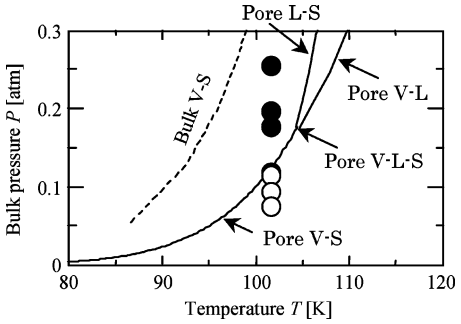

Figure 4. MD results of p-T relation for pore fluid superimposed on bulk phase boundary (broken line). Open circles show the surface adsorption, and closed circles the solid state. Also drawn are estimated phase boundaries for pore fluid (solid lines).

and Δs is the difference in entropy. k is the Boltzmann constant.

The following Clausius-Clapeyron equation of the bulk fluid was applied to the description of the sublimation phenomenon of pore fluid. Although this type of treatment in pressure is not scientifically correct in nanopores, our aim is to obtain a simple model for understanding and estimating the sublimation points in pores. Sublimation point B was explained as a shift from the triple point of pore fluid.

$$\ln \frac{p|_B}{p|_A} = -\frac{\Delta h}{k}\left(\frac{1}{T|_B} - \frac{1}{T|_A}\right) \tag{3}$$

where Δh is the latent heat. Using the physical properties of LJ-methane clarified by Kofke, the $p - T$ relationship of sublimation is predicted by our model for the pore width examined here. Figure 4 shows the MD results (circles) to be compared with the prediction by Eq. (3) (solid line). Open circles show the surface adsorption, and closed circles the solid state. The broken line is Kofkes' coexistence curve (Kofke, 1993; Agrawal and Kofke, 1995) of LJ-methane for the bulk. Our model successfully explains the sublimation point with reasonably good performance.

4. Lennard-Jones Phase Diagram in Slit Nanopores

This section describes the procedure for predicting a whole Lennard-Jones phase diagram in slit-shaped nanopores. First, to identify the pore wall potential, a standard adsorption isotherm should be measured for a non-porous solid with similar composition to that of the porous material in question. The adsorbate-solid interaction strength can be obtained in terms of the parameter C in the following FHH-like equation, through a fitting with experimental adsorption thickness t (Kanda et al., 2000c).

$$kT \ln \frac{p}{p_s} = -\frac{C}{t^3} \tag{4}$$

Using C, the capillary coexistence condition can be calculated by the following equation (Miyahara et al., 1997), in which adsorbate-solid interaction is considered in addition to the Kelvin effect.

$$\begin{aligned} kT \ln \frac{p}{p_s} &= \Delta\psi(x) - v_L \frac{\gamma_{gl}}{\rho(x)} \\ &= -C\left(\frac{1}{(H/2+x)^3} + \frac{1}{(H/2-x)^3}\right) \\ &\quad - v_L \frac{\gamma_{gl}}{\rho(x)} \end{aligned} \tag{5}$$

$\rho(x)$ is the local curvature of condensate, which does not stay constant because of the pore-wall potential. Geometrical integration of Eq. (5) gives a whole meniscus shape, which corresponds to H for given T and p. For a given H, one can thus find the $p - T$ relation, which represents the capillary (V-L) coexistence.

The procedure for calculating the shift in freezing point consists of two steps. First, for pore fluid in equilibrium with *saturated* vapor in bulk, a compression effect by strong interaction from pore walls increases the freezing point of pore fluid as shown in Eq. (6) (Miyahara and Gubbins, 1997).

$$\frac{T_a - T_f}{T_f} = -\frac{\Delta\psi(0)}{\Delta h} = -\frac{C}{\Delta h}\frac{2}{(H/2)^3} \tag{6}$$

In the case that pore fluid equilibrates with unsaturated vapor, the pressure of pore fluid becomes negative due to the Laplace effect. Application of the p-T relation (the Clapeyron equation) to pore fluid gives a shift of freezing point from T_a. Simultaneous equations of the Laplace equation and Clausius-Clapeyron equation describe the significant change of freezing point against vapor phase pressure as shown by "pore S-L" in Fig. 5 (Miyahara et al., 2000a).

$$p = p_s(T) \exp\left[-\left(\frac{\Delta s}{\Delta v}\right)_{\text{bulk}} \frac{v_L}{kT}(T_a - T)\right] \tag{7}$$

The simultaneous solution of Eqs. (5) and (7) gives the triple point (Eqs. (1) and (2)). With the sublimation

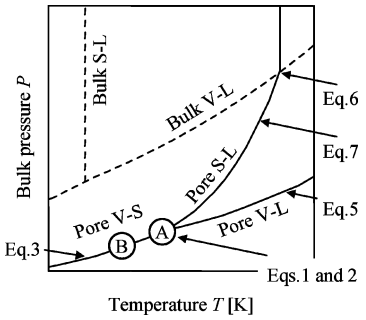

Figure 5. Schematic phase diagram for model consideration. Point A indicates a triple point in a pore. Point B.

curve of Eq. (3), the above series of equations yields the whole LJ phase diagram in slit-shaped nanopores.

5. Conclusion

Sublimation points in nanopores were examined employing an MD technique, which was able to simulate the pore fluid with its bulk equilibrium pressure specified. The technique successfully determined the sublimation points, or solid-vapor transition point, in nanopores located on the bulk phase diagram. The sublimation pressure was significantly lower than the bulk sublimation pressure, or the sublimation temperature must be considerably higher than the bulk. A simple model to describe sublimation points was derivedas the shift from the previously reported triple point of pore fluid by the authors. The model showed good agreement with the MD results, thus proving its reliability. With this agreement, a whole LJ phase diagram in slit-shaped nanopores can now be predicted.

References

Agrawal, R. and D.A. Kofke, *Mol. Phys.*, **85**, 43–59 (1995).
Kanda, H., M. Miyahara, and K. Higashitani, *Langmuir*, **16**, 6064–6066 (2000a).
Kanda, H., M. Miyahara, and K. Higashitani, *Langmuir*, **16**, 8529–8535 (2000b).
Kanda, H., M. Miyahara, T. Yoshioka, and M. Okazaki, *Langmuir*, **16**, 6622–6627 (2000c).
Kanda, H., M. Miyahara, and K. Higashitani, *J. Chem. Phys.*, **120**, 6173–6179 (2004).
Kirkwood, J.G. and F.P. Buff, *J. Chem. Phys.*, **17**, 338–343 (1949).
Kofke, D.A., *J. Chem. Phys.*, **98**, 4149–4162 (1993).
Maddox, M.W. and K.E. Gubbins, *J. Chem. Phys.*, **107**, 9659–9667 (1997).
Melrose, J.C., *Ind. and Eng. Chem.*, **60**, 53–70 (1968).
Miyahara, M. and K.E. Gubbins, *J. Chem. Phys.*, **106**, 2865–2880 (1997).
Miyahara, M., H. Kanda, M. Shibao, and K. Higashitani, *J. Chem. Phys.*, **112**, 9909–9916 (2000a).
Miyahara, M., H. Kanda, T. Yoshioka, and M. Okazaki, *Langmuir*, **16**, 4293–4299 (2000b).
Miyahara, M., T. Yoshioka, and M. Okazaki, *J. Chem. Phys.*, **106**, 8124–8134 (1997).
Patrik, W.A. and W.A. Kemper, *J. Phys. Chem.*, **42**, 369–380 (1938).
Tolman, R.C., *J. Chem. Phys.*, **16**, 758–774 (1948).